FAST ANGLES-ONLY INITIAL RELATIVE ORBIT DETERMINATION FOR ONBOARD APPLICATION

Jean-Sébastien Ardaens* **and Gabriella Gaias†**

This paper presents three computationally-light algorithms to solve the initial relative orbit determination problem using line-of-sight measurements. A comparative assessment of their performance and robustness is made, based on real flight data from two different in-orbit experiments. The proposed algorithms are optimized for the challenging scenario of far-range noncooperative rendezvous in low Earth orbits.

INTRODUCTION

Angles-only relative navigation has been deeply investigated over the past years at the German Space Operations Center (DLR/GSOC), resulting in the realization of two in-orbit demonstrations. The ARGON (Advanced Rendezvous demonstration using GPS and Optical Navigation) experiment[1] was conducted in 2012 using the PRISMA formation-flying testbed[2] and demonstrated far- to mid-range ground-in-the-loop approach to a noncooperative target using optical methods. Based on the resulting experience, a more challenging experiment called AVANTI[3] (Autonomous Vision Approach Navigation and Target Identification) was successfully executed in autumn 2016 to demonstrate the ability to autonomously rendezvous with a noncooperative target using solely optical measurements. AVANTI was implemented on the German BIROS satellite[4] and used a picosatellite[5] (which had been previously released in orbit by BIROS) as noncooperative target for the sake of the experiment.

Both in-orbit demonstrations greatly differed in terms of complexity, implementation and operational conditions but also in terms of constraints posed to the relative navigation. Contrary to ARGON which, thanks to the dawn-dusk orbit of PRISMA, benefited from optimal illumination conditions, AVANTI was dealing with target objects flying on any kind of low Earth orbit. This had dramatic impacts in terms of visibility because the picosatellite was only visible at one single location of the orbit, for a very short time (10 minutes) so that only a tiny part of the relative motion could be observed. Furthermore, BIROS was orbiting at a lower altitude (500 km against 750 km for PRISMA) inducing a strong unknown differential drag which had to be estimated as part of the navigation process.

During AVANTI and ARGON, the relative navigation task was performed by the means of nonlinear estimation techniques (nonlinear least-squares on ground[6] and extended Kalman filter on board[7]). Both methods require the use of a coarse guessed solution around which the quantities are linearized. Dealing with a known target, this a priori information was provided at that time by the means of Two-Lines Elements (TLE).

*Reasearch Engineer, GSOC/Space Flight Technology, Muenchener Str. 20, 82234 Wessling, Germany.
†Dr., DAER - Politecnico di Milano, Via La Masa 34, 20156 Milano, Italy.

In order to simplify the interfaces and operations, it might be, however, desirable to replace the use of TLEs by an angles-only Initial Relative Orbit Determination (IROD) algorithm able to compute this coarse solution using only bearing observations. This is not a trivial task because the problem is weakly observable. Numerous research activities have already been conducted to improve the observability, for example by the means of maneuvers, using a camera offset or by improving the measurement equations and/or relative dynamics.[8–14] Several authors have also specifically tackled the problem of IROD using dedicated algorithms.[15–17]

Recently, an alternative method has been developed by the authors to solve the angles-only IROD problem based on a simple but effective numerical approach. This method, intended for far-range rendezvous on near-circular low Earth orbits, is shown to be very robust, thus particularly suited for sparse and noisy measurements, and could be successfully validated on real data sets coming from the ARGON and AVANTI experiments.[18] However, the underlying algorithm is computationally expensive and not well adapted for an onboard implementation. The paper intends to investigate if some optimization can be done to accelerate the delivery of results. After recalling in the first Section the core principles of the method described in Reference 18, the paper presents in the second Section three alternative algorithms to reduce the computational time. Finally, the algorithm performance is assessed using real and simulated data.

NUMERICAL SOLUTION TO THE IROD PROBLEM

As already addressed in the literature, the angles-only relative navigation problem is not observable using a linear framework.[8] Thus there exists an infinity of solutions matching a given set of angles-only observations. If $\boldsymbol{x}(t_0)$ denotes a relative state vector at time t_0 leading to a given measurement profile, the scaled state vector $\mu\boldsymbol{x}(t_0)$ is also a solution. In reality, the problem is not linear. Consequently, small discrepancies will appear when trying to fit an arbitrary scaled solution $\mu\boldsymbol{x}(t_0)$ with a given set of measurements using nonlinear relative motion and measurement models, and these errors will grow as the scale factor μ moves away from the real scaling factor $\hat{\mu}$. The algorithm described in Reference 18 performs a series of orbit determinations at different scaling factors μ within a given interval. As depicted in Figure 1, if σ denotes the standard deviation of the fitting residuals, a residual function is obtained which reaches its minimum for the true scaling factor $\hat{\mu}$, allowing solving for the range ambiguity.

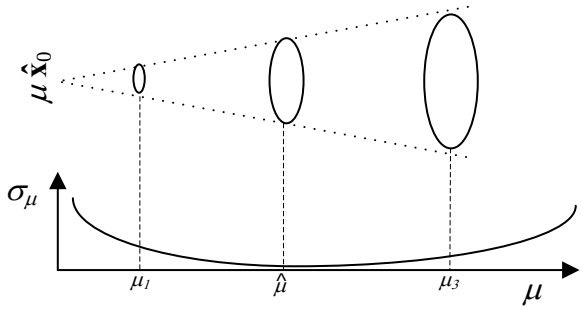

Figure 1. Fitting residuals corresponding to a series of least-squares adjustments in the vicinity of the linear solutions $\mu\hat{x}_0$, which are schematically represented by ellipses on top of the graph.

This behavior can be intuitively well understood but is in fact not obvious. Thus, a mathematical demonstration is provided in Reference 18 to demonstrate that the equivalent function $m(\mu) = n\sigma_\mu^2$,

n being the number of measurements, is convex for the problem under consideration (*i.e.*, far-range rendezvous in low Earth near-circular orbit). This is done by deriving an approximate value for $m(\mu)$:

$$m(\mu) = \boldsymbol{b}_1^T \boldsymbol{M} \boldsymbol{b}_1 + \mu^2 \boldsymbol{b}_2^T \boldsymbol{M} \boldsymbol{b}_2 + 2\mu \boldsymbol{b}_1^T \boldsymbol{M} \boldsymbol{b}_2, \tag{1}$$

where $\boldsymbol{b}_1$, $\boldsymbol{b}_2$, and $\boldsymbol{M}$ are quantities that depend on the measurements and relative dynamics (see Reference 18 for more details). The convexity of the function $m(\mu)$ is verified using the second order derivative, which is positive because $\boldsymbol{M}$ is semi-definite positive, yielding $\frac{d^2 m(\mu)}{d\mu^2} = \boldsymbol{b}_2^T \boldsymbol{M} \boldsymbol{b}_2 \geq 0$. Consequently, the minimum function is convex and reaches its minimum for

$$\hat{\mu} = -\frac{\boldsymbol{b}_1^T \boldsymbol{M} \boldsymbol{b}_2}{\boldsymbol{b}_2^T \boldsymbol{M} \boldsymbol{b}_2}. \tag{2}$$

FAST ALTERNATIVE IROD ALGORITHMS

Binary Search

The convexity of the residual function makes it possible to replace the systematic search by a faster algorithm, based on gradient descent or binary search. In view of the flatness of the curve, it is considered more robust to use a binary search to find the minimum of the residual function. The algorithm is very simple: starting from an interval $I_0 = [\mu_\mathrm{A}, \mu_\mathrm{B}]$, the derivative $m'(\mu)$ is evaluated at the points μ_A and $\mu_k = \frac{1}{2}(\mu_\mathrm{A} + \mu_\mathrm{B})$. The computation of $m'(\mu)$ is done numerically by evaluating the minimum at μ and $\mu + h$ with $h \ll \mu$. The objective is to find an interval over which the sign of the derivative changes. Thus, if $m'(\mu_\mathrm{A}) m'(\mu_k) < 0$, the interval will be restricted in the next iteration to $I_k = [\mu_\mathrm{A}, \mu_k]$ otherwise to $I_k = [\mu_k, \mu_\mathrm{B}]$. The iteration stops if the size of the interval becomes smaller than a user-defined threshold. Consequently, four evaluations of $m(\mu)$ are required at each step but, because a solution is expected to be found within a few steps, a substantial reduction of the number of relative orbit determinations is still achieved compared to the systematic search. Obviously, a nonlinear least-squares estimation based on an analytical model of the relative motion is mandatory when evaluating $m(\mu)$ to reduce the computational efforts. In order to further optimize the computational load, the approximate solution for $m(\mu)$ provided by Eq. 1 can be used instead of the nonlinear least-squares estimate. The computational complexity of both methods is similar to retrieve the least-squares solution. However the nonlinear approach will typically require several iterations to achieve the convergence while the solution given by Eq. 1 will be faster.

Exploiting the Model of the Residual Curve

The mathematical framework developed Reference 18 may also be used to derive faster analytical methods. The most obvious approach consists in using Eq. 2 in an iterative way. Starting from an arbitrary μ_1, a value for $\hat{\mu}$ is obtained. This value might not be accurate enough because of the linearizations and approximations assumed when deriving Eq. 2. Thus, an updated value for the global minimum can be obtained by starting with $\mu_2 = \hat{\mu}$. The iterative process stops when the computed correction drops below a user-defined threshold.

Linear Matrix Method

The third and last approach is not based anymore on the model of the residual curve but takes advantage from the fact that a quadratic relation had been derived for the measurement equation in Reference 18. If $\{\boldsymbol{u}_i\}$ corresponds to a given set of n line-of-sight measurements taken at times t_i

and $\boldsymbol{r}(t_i)$ represents the relative position vector at the corresponding times, the general expression for the measurement equation in the absence of measurement noise is:

$$\boldsymbol{u}_i \times \boldsymbol{r}(t_i) = 0, i \in [1, n]\,. \tag{3}$$

Following Reference 18, this expression can be approximated as a quadratic expression:

$$\boldsymbol{u}_i \times \left(\boldsymbol{\Phi}_{1\text{-}3,1\text{-}6}\boldsymbol{x}_0 - \frac{1}{2R} \begin{pmatrix} 1 \\ 0 \\ 0 \end{pmatrix} \boldsymbol{x}_0^T \boldsymbol{\Phi}_{2,1\text{-}6}^T \boldsymbol{\Phi}_{2,1\text{-}6}\boldsymbol{x}_0 \right) = 0, i \in [1, n] \tag{4}$$

where $\boldsymbol{x}_0$ is the initial relative state vector at time t_0 using a curvilinear Cartesian representation, $\boldsymbol{\Phi}$ is the state transition matrix using the Gim-Alfriend model,[19] and R is the radius of the orbit.

This quadratic expression can be solved using the method provided in Reference 20, which consists in creating a 27-dimensional vector $\boldsymbol{\chi}$ comprising the state vector $\boldsymbol{x}$ augmented by all the possible quadratic combinations of its components. If x_i denotes the i^{th} component of $\boldsymbol{x}$, $\boldsymbol{\chi}$ can be written in the form of:

$$\boldsymbol{\chi} = \begin{pmatrix} x_1 & ... & x_6 & x_1x_1 & x_1x_2 & ... & x_6x_6 \end{pmatrix}^T. \tag{5}$$

Eq. 4 can be rewritten using this new variable:

$$\boldsymbol{a}_1x_1 + ... + \boldsymbol{a}_6x_6 + \boldsymbol{a}_{11}x_1^2 + \boldsymbol{a}_{12}x_1x_2 + \boldsymbol{a}_{66}x_6^2 = 0, i \in [1, n] \tag{6}$$

where $\boldsymbol{a}_i$ is a 3-dimensional vector. By accumulating n measurements, a linear system is obtained:

$$\boldsymbol{A}\boldsymbol{\chi} = 0. \tag{7}$$

Thus the solution of this linear problem belongs to the null space of $\boldsymbol{A}$. If $\hat{\boldsymbol{\chi}}$ is a solution of $\boldsymbol{A}$, then $\alpha\hat{\boldsymbol{\chi}}$ belongs as well to the null space. It is now possible to exploit the fact that the components of $\boldsymbol{\chi}$ are not independent to solve for the scaling factor α. In fact, the 7^{th} component of $\boldsymbol{\chi}$ has to be the square of the 1^{st} component, etc. Thus, a solution to the problem must have the form:

$$\boldsymbol{\chi} = \begin{pmatrix} \alpha\hat{\chi}_1 & ... & \alpha\hat{\chi}_6 & \alpha^2\hat{\chi}_1^2 & \alpha^2\hat{\chi}_1\hat{\chi}_2 & ... & \alpha^2\hat{\chi}_6\hat{\chi}_6 \end{pmatrix}^T. \tag{8}$$

Using this formulation, Eq. 7 becomes

$$\alpha\boldsymbol{A}_{1-3n,1-6} \begin{pmatrix} \hat{\chi}_1 \\ \hat{\chi}_1 \\ ... \\ \hat{\chi}_6 \end{pmatrix} + \alpha^2\boldsymbol{A}_{1-3n,7-27} \begin{pmatrix} \hat{\chi}_1\hat{\chi}_1 \\ \hat{\chi}_1\hat{\chi}_2 \\ ... \\ \hat{\chi}_6\hat{\chi}_6 \end{pmatrix} = 0 \tag{9}$$

which can be rewritten in the form:

$$\alpha\boldsymbol{q} + \alpha^2\boldsymbol{p} = 0. \tag{10}$$

Excluding the trivial solution, α can finally be solved in the least-squares sense with:

$$\alpha = -\frac{\boldsymbol{p}^T\boldsymbol{q}}{\boldsymbol{p}^T\boldsymbol{p}}. \tag{11}$$

Ideally, the null space corresponds to an eigenvalue equal to zero. Reference 20 indicates that, in the presence of sensor noise, values slightly different from zero might be obtained. Thus, Reference 20 advises to use a Singular Value Decomposition and to systematically compute 27 values of α corresponding to the 27 eigenvectors, yielding 27 different solutions. The final solution is obtained by computing the measurement residuals associated to each solution and retaining the solution yielding the smallest residuals.

PERFORMANCE ASSESSEMENT

The flight data from the three scenarios already employed in Reference 18 are used for performance assessment. Their main characteristics are quickly recalled here for completeness:

- **ARGON 5h**: Data set from the ARGON experiment. The Mango satellite (chaser) observes the Tango spacecraft (target) during 5h (or 3 orbits) using a far-range camera. Both satellites are flying on a Sun-synchronous dawn-dusk near-circular orbit at 750 km altitude. No maneuver is executed during this time interval. The chaser and target are separated by 30 km.
- **ARGON 14h**: Same mission but the data set now spans 14 h (April 25$^{\text{th}}$ 2012, from 2:00 to 16:00 UTC) and is also free from maneuvers. At that time, the chaser and target are separated by 23.5 km.
- **AVANTI 18h**: Data set from the AVANTI experiment. The collection of observations starts on October 20$^{\text{th}}$, 2016 22:00 UTC when the BIROS satellite (chaser) and BEESAT-4 (target) are separated by 45 km. The intersatellite distance rapidly decreases during the time interval due to the large initial relative semi-major axis (80 m). Because of the poor visibility conditions encountered during AVANTI, 10 minutes of observations are available every orbits. The formation undergoes in addition a much stronger differential drag due to the lower altitude and the very different ballistic coefficients of the chaser and target.

The performance of the algorithms is summarized in Table 1. For each scenario, the reference based on an external independent sensor as well as the solution found in Reference 18 using the time consuming series of least-squares are recalled to ease the comparison. The binary search method is performed using the nonlinear least-squares estimation of $m(\mu)$ and with the approximate value of $m(\mu)$ obtained using the linear least-squares solution of Eq. 1. Finally, the methods based on the quadratic modeling of the linear curve and based on the Linear Matrix Method (LMM) are investigated.

The computational time required by each method is coarsely evaluated on a desktop equipped with a Core i5 processor and is only intended to provide an order of magnitude. Depending on the target computer, these values might be be much larger in case of spaceborne embedded application.

Some observations can already be drawn. All methods yield similar solutions for the ARGON scenarios, except for the LMM which results in a degraded solution in the 5h-long case. The curve modeling and LMM are two orders of magnitude faster than the series of least-squares, but failed to find a solution in the AVANTI case. Being based on exactly the same model as the series of least-squares approach, the nonlinear binary search yields almost identical results but is about one order of magnitude faster. The linear binary search is even faster but provides a degraded solution for the AVANTI case.

Obviously, the AVANTI case is more challenging for the IROD methods. With respect to the ARGON cases, two major differences are affecting this scenario: a large unknown differential drag which is not taken into account by the models and very sparse measurements. In order to better isolate the contribution of these effects, two additional scenarios are simulated in the sequel. The first one consists of the 14h-ARGON case, for which only 10 minutes of measurements per orbit have been retained to simulate poor visibility conditions. The second one consists of the AVANTI scenario completed with additional simulated measurements, as if a dusk-dawn orbit was used. Table 2 summarizes the IROD performance obtained using these simulated cases.

Table 1. Performance comparison of the different methods applied to real in-orbit scenarios

	Method	Solution [m]	Time [s]
ARGON 5h	Reference	[-21 -29568 -51 -395 -4 295]	-
	Series of least-squares	[-20 -32000 -55 -429 -4 317]	51
	Binary search (nonlinear)	[-20 -32100 -55 -429 -5 318]	8
	Binary search (linear)	[-20 -32100 -53 -431 -6 325]	3
	Curve modeling	[-23 -30000 -50 -401 -5 302]	0.6
	Linear matrix method	[-26 -24000 -80 -311 -5 240]	0.4
ARGON 14h	Reference	[-131 -23650 -20 -303 -4 247]	-
	Series of least-squares	[-139 -25000 -21 -315 -5 257]	70
	Binary search (nonlinear)	[-139 -24800 -21 -316 -5 258]	10
	Binary search (linear)	[-138 -24800 -20 -318 -6 263]	7
	Curve modeling	[-138 -24700 -20 -316 -6 261]	0.7
	Linear matrix method	[-133 -24700 -20 -316 -6 261]	0.6
AVANTI 18h	Reference	[84 44786 155 609 -8 714]	-
	Series of least-squares	[68 39000 137 533 -10 625]	11
	Binary search (nonlinear)	[65 38000 132 522 -6 604]	2
	Binary search (linear)	[56 31888 113 419 -3 500]	0.3
	Curve modeling	failed	-
	Linear matrix method	failed	-

Table 2. Performance comparison of the different methods applied to simulated scenarios

	Method	Solution [m]	Time [s]
ARGON poor visibility	Reference	[-131 -23650 -20 -303 -4 247]	-
	Series of least-squares	[-139 -25000 -19 -320 -5 257]	6.4
	Binary search (nonlinear)	[-137 -24800 -19 -319 -5 256]	1.2
	Binary search (linear)	[-157 -27861 -21 -349 -6 290]	0.2
	Curve modeling	[-143 -25617 -19 -326 -6 267]	0.04
	Linear matrix	failed	-
AVANTI full visibility	Reference	[84 44786 155 609 -8 714]	-
	Series of least-squares	[72 43000 149 589 -7 692]	276
	Binary search (nonlinear)	[72 42900 149 589 -7 692]	60
	Binary search (linear)	[77 44473 157 607 -3 704]	40
	Curve modeling	[77 44200 157 604 -3 701]	8
	Linear matrix	[86 46400 161 620 -4 730]	1.9

The simulated ARGON case with reduced visibility posed some difficulties to the LMM, and to a lesser extent, to the linear binary search. Reciprocally, all methods are properly working for the AVANTI case with full visibility, which tends to indicate that the limited visibility is the main reason for the degraded performance and failure of some methods rather than the unmodeled differential drag. There is no obvious explanation for the degraded behavior in case of poor visibility. One hypothesis is that the linear mapping between mean and osculating elements within the underlying Gim-Alfriend model introduces some errors, which compensate when observing the full relative motion but introduce nonrecoverable systematic errors when observing only a small part of the motion.

CONCLUSION

Three alternative algorithms for Initial Relative Orbit Determination (Binary Search, Curve Modeling, Linear Matrix) have been developed to reduce the computational load of the numerical method based on a series of least-squares adjustments. The gain of speed greatly differs between the algorithms. While the Binary Search uses the core principle of the original computationally-heavy algorithm and thus shows a moderate time improvement (factor 5 to 10), the Curve Modeling and Linear Matrix Method use directs methods that lead to a dramatic reduction of computational time (by two orders of magnitude).

The success and performance of the alternative methods is, however, not always guaranteed. Even if no formal demonstration could be derived at this stage, the probability of failure seems to be correlated with the visibility of the relative motion and could be due to some deficiencies of the relative motion and measurement models. Thus, some care has to be taken when utilizing these fast methods. The binary search based on nonlinear least-squares estimation seems to be for the moment the best compromise for onboard applications, combining good performance and robustness. Future work will investigate if the fastest methods can be made more robust by improving the models.

ACKNOWLEDGMENT

The construction of the BIROS satellite was funded by the Federal Ministry of Education and Research of Germany (BMBF) (project number FKZ 01LK0904A).

REFERENCES

[1] S. D'Amico, J.-S. Ardaens, G. Gaias, H. Benninghoff, B. Schlepp, and J. L. Jørgensen, "Noncooperative Rendezvous Using Angles-Only Optical Navigation: System Design and Flight Results," *Journal of Guidance, Control, and Dynamics*, Vol. 36, No. 6, 2013, pp. 1576–1595. doi: 10.2514/1.59236.

[2] S. Persson, B. Jakobsson, and E. Gill, "PRISMA - Demonstration Mission for Advanced Rendezvous and Formation Flying Technologies and Sensors," No. 05-B56B07, Fukuoka, Japan, 56th International Astronautical Congress, 2005.

[3] G. Gaias and J.-S. Ardaens, "Flight Demonstration of Autonomous Noncooperative Rendezvous in Low Earth Orbit," *Journal of Guidance, Control, and Dynamics*, Vol. 41, No. 6, 2018, pp. 1137–1354. https://doi.org/10.2514/1.G003239.

[4] W. Halle, W. Bärwald, T. Terzibaschian, M. Schlicker, and K. Westerdorf, "The DLR -Satellite BIROS in the Fire-Bird Mission," *Proceedings of the 4S Symposium: Small Satellites, Systems and Services*, Noordwijk, The Netherlands, 26 - 30 May 2014, Majorca, Spain, European Space Agency, 2014.

[5] F. Baumann, S. Trowitzsch, and K. Brieß, "BEESAT - A CubeSat Series Demonstrates Novel Picosatellite Technologies," Brussels, Belgium, 4th European CubeSat Symposium, 2012.

[6] J.-S. Ardaens and G. Gaias, "Angles-Only Relative Orbit Determination in Low Earth Orbit," *Advances in Space Research*, Vol. 31, No. 11, 2018, pp. 2740–2760. 10.1016/j.asr.2018.03.016.

[7] J.-S. Ardaens and G. Gaias, "Flight Demonstration of Spaceborne Real-Time Angles-Only Navigation to a Noncooperative Target in Low-Earth Orbit," *Acta Astronautica*, Vol. 153, 2018, pp. 367–382. 10.1016/j.actaastro.2018.01.044.

[8] D. C. Woffinden and D. K. Geller, "Optimal Orbital Rendezvous Maneuvering for Angles-Only Navigation," *Journal of Guidance, Control, and Dynamics*, Vol. 32, No. 4, 2009, pp. 1382–1387.

[9] G. Gaias, S. D'Amico, and J.-S. Ardaens, "Angles-Only Navigation to a Noncooperative Satellite Using Relative Orbital Elements," *Journal of Guidance, Control, and Dynamics*, Vol. 37, No. 2, 2014, pp. 439–451. doi: 10.2514/1.61494.

[10] J. Grzymisch and W. Fichter, "Analytic Optimal Observability Maneuvers for In-Orbit Bearings-Only Rendezvous," *Journal of Guidance, Control, and Dynamics*, Vol. 37, No. 5, 2014, pp. 1658–1664. doi: 10.2514/1.G000612.

[11] J. Grzymisch and W. Fichter, "Observability Criteria and Unobservable Maneuvers for In-Orbit Bearings-Only Navigation," *Journal of Guidance, Control, and Dynamics*, Vol. 37, No. 4, 2014, pp. 1250–1259. doi: 10.2514/1.62476.

[12] D. K. Geller and I. Klein, "Angles-Only Navigation State Observability During Orbital Proximity Operations," *Journal of Guidance, Control, and Dynamics*, Vol. 37, No. 6, 2014, pp. 1976–1983. doi: 10.2514/1.G000133.

[13] A. C. Perez, *Applications of Relative Motion Models Using Curvilinear Coordinate Frames*. PhD thesis, Utah State University, U.S.A, 2017.

[14] T. A. Lovell and S. G. Tragesser, "Guidance for Relative Motion of low Earth Orbit Spacecraft based on Relative Orbit Elements," No. 04-4988, Providence, Rhode Island, USA, AIAA Guidance, Navigation and Control Conference and Exhibit, 2004.

[15] S. Garg and A. Sinclair, "Initial Relative-Orbit Determination Using Second-Order Dynamics and Line-of-Sight Measurements," Williamsburg, Virginia, 25th AAS/AIAA Space Flight Mechanics Meeting, 2015.

[16] D. K. Geller and T. A. Lovell, "Angles-Only Initial Relative Orbit Determination Performance Analysis using Cylindrical Coordinates," *The Journal of the Astronautical Sciences*, Vol. 64, 9 2017, pp. 72–96, 10.1007/s40295-016-0095-z.

[17] J. Sullivan, A. Koenig, and S. D'Amico, "Improved Maneuver-Free Approach to Angles-Only Navigation for Space Rendezvous," No. 16-530, Napa, California, 26th AAS/AIAA Space Flight Mechanics Conference, 2016.

[18] J.-S. Ardaens and G. Gaias, "A Numerical Approach to the Problem of Angles-Only Initial Relative Orbit Determination in Low Earth Orbit," *Advances in Space Research*, 2019. 10.1016/j.asr.2019.03.001.

[19] D.-W. Gim and K. T. Alfriend, "State Transition Matrix of Relative Motion for the Perturbed Noncircular Reference Orbit," *Journal of Guidance, Control and Dynamics*, Vol. 26, No. 6, 2003, pp. 956–971.

[20] D. A. Cicci, "Spacecraft Formation Control and Estimation via Improved Relative-Motion Dynamics," Final Report AFRL-RV-PS-TR-2017-0052, Auburn University, Auburn, AL, 2017.